

UNCLASSIFIED

AD NUMBER
ADB232385
NEW LIMITATION CHANGE
TO Approved for public release, distribution unlimited
FROM Distribution: Further dissemination only as directed by Office of Naval Research, 800 N. Quincy St., Arlington, VA 22217-5660, Jan 98 or higher DoD authority.
AUTHORITY
Office of Naval Research ltr dtd 10 Jun 98

THIS PAGE IS UNCLASSIFIED

FINAL REPORT

CLEAN, AGILE PROCESSING TECHNOLOGY

Contract # N00014-96-C-0139

PI: S. W. Sinton
Co-PI: A. W. Chow
Lockheed Martin Missiles & Space
Advanced Technology Center
3251 Hanover St.
Palo Alto, CA 94043
Office: (415) 424-2532
FAX: (415) 354-5795
steve.sinton@lmco.com

DISTRIBUTION STATEMENT F: Further dissemination only as directed by
authority. ONR 1-98 or higher DoD

800 N. Quincy St.
Arlington, VA 22217-5660

19980105 055

PROGRAM OBJECTIVES & GOALS

This contract was part of the "Clean, Agile Manufacturing of Explosives " (CAME) program managed by ONR and funded by the Strategic Environmental Research and Development Program (SERDP). The overall goal of CAME was to enable a 90% reduction in pollution from the Nation's propellants, explosives, and pyrotechnics (PEP) life cycle. Major elements of CAME designed to address the pollution reduction goal were the reduction or elimination of manufacturing scrap and the development of recycle and/or recovery methods for PEP materials. The CAME effort at Lockheed Martin Missiles & Space (LMMS) focused on a selected process with the aim of understanding how the physical/chemical behavior of a plastic-bonded explosive (PBX) in the process affects the scrap and pollution generated by the process. Specifically, LMMS utilized rheology and magnetic resonance imaging (MRI) to study the flow of suspensions to model PBX injection loading operations developed at Naval Surface Weapons Center-Indian Head Division (NSWC) for BLU-97 submunitions. We examining how suspensions flow through the injection loader geometry and helped identify process conditions that lead to undesirable scrap or defective submunitions. In this manner, the LMMS project addressed the primary CAME goal of pollution reduction through inherently cleaner processes.

This LMMS effort was closely aligned with related programs at other sites involved in the SERDP-sponsored research on the processing science of energetic materials. These groups included the NSWC, Stevens Institute of Technology (SIT), Los Alamos National Laboratory (LANL), Sandia National Laboratory, the California Institute of Technology (CIT), the Massachusetts Institute of Technology (MIT), and the Naval Air Warfare Center (NAWC), China Lake.

SUMMARY OF RESULTS

The two primary process parameters measured in the NSWC BLU-97 process were injector pressure and piston speed. NSWC identified certain conditions in these parameters which indicated "particle jamming" as a probable cause for inhomogeneities and voids in some munition products. However, these process parameters alone do not give sufficient information to identify the source of product deficiencies. Furthermore, in a study done by NSWC and Sandia National Laboratory, it was determined that advanced process control algorithms operating solely on pressure and piston speed would not ensure reject-free products. More information about what actually occurs in the injection loader and the nature of the "particle jamming" phenomenon was sought.

We built a model of the NSWC injection loader for controlled studies of the process with model suspensions. This one-half-scale mockup allows various contraction geometries and contraction ratios to be tested. The mockup was also designed to be compatible with the LMMS magnetic resonance imaging (MRI) system. By running the process while the system is installed in the MRI instrument we could observe changes in the suspension and correlate those changes with the process parameters. In this way we can for the first time identify the phenomena responsible for uncontrolled variations in munition quality. These topics are summarized below.

Our model injection loader consists of an epoxy-fiber overwrapped plastic tube for the main pressure vessel and various interchangeable contraction throats. Fiber overwrapping is necessary to fortify the tube against the high internal pressures (up to 1000 psi) anticipated as a result of the scaled-down injector throat. Other components (e.g. piston) are also made from non-metallic parts to allow magnetic resonance images to be obtained as the suspension is processed.

Processing experiments were performed to identify the conditions which cause unstable suspension flows associated with the processing problems. Our results are in general agreement with the observations from the NSWC BLU-97 process. One major difference is that in our model system we are using a density-matched suspension whereas particle settling is known to occur with the BLU-97 propellant (PBXN-107). The fact that unstable flows are observed with a density-matched suspension indicates that particle settling is not a required aspect of processing problems. The relative importance of particle settling could be addressed by varying the suspending liquid's density relative to the particle density. Real-time pressure measurements were collected in a set of experiments designed to determine the effects of particle concentration, bulk flow rate, and base fluid viscosity.

The model suspension was imaged in the contraction region both early in the flow, when the pressure-time trace is smooth and stable, and later when pressure suddenly rises and begins to fluctuate (the conditions associated with unstable flows). These images indicate that the average concentration of particles in the contraction has not changed drastically, but that the *texture* of the local particle concentration variations is different. At the point where pressure is relatively high and fluctuating, the image appears grainier and there is evidence for larger aggregates of particles than for the early-time (low pressure) situation. A statistical analysis was performed on the images, and the results support these conclusions.

DETAILED DESCRIPTION OF PROGRAM RESULTS

MODEL INJECTION LOADER DESIGN

The model injection loader system was designed to meet the following requirements.

- The system was intended to model an injection loader system which involves piston-driven flow from a cylindrical reservoir through a contraction. A one-half scaling of the NSWC system was required to accommodate the MRI RF probe and magnet. The magnet is 150-mm, vertical-bore superconducting unit with a central field of 4.7-Tesla. The probe internal diameter can accommodate a tube with an outer diameter of 68 mm.
- The piston, reservoir, contraction, and outflow tube all had to be of non-magnetic, non-conducting materials to allow MRI.
- The system had to be capable of withstanding a maximum pressure drop of 1000 psi (as measured in the piston reservoir). Real-time pressure measurement was required.
- The outflow region had to be modular to allow swapping of different contraction geometries.
- The piston drive motor had to be placed at a sufficient distance from the magnet center to avoid any undesirable interactions between motor parts and magnet. A variable speed motor was required to facilitate studies as a function of flow rate. Typically, the system was run at constant flow rate (piston speed), but, with modification, constant pressure studies are possible.
- The entire system had to be supported independently of the magnet so that piston forces would not be applied to the magnet. The support structure had to include an adjustable height capability to allow imaging of the entire reservoir and outflow geometry.

An overall schematic of the system is shown in Figure 1. The magnet is surrounded by a support frame composed of 3-in by 3-in square aluminum tubes and connecting brackets. (For clarity, the magnet legs and base are not depicted in Figure 1.) The piston drive train sits atop this frame. It consists of a variable speed electric motor and worm-gear assembly which drives a leadscrew-follower arrangement. The leadscrew follower forces a long aluminum push rod down on the piston inside the magnet. The push rod was sized appropriately to avoid buckling. Total distance between motor and magnet center is about 90 inches; tests indicated no major effect on magnet shimming with this arrangement. An in-line force transducer (Sensotec button load cell, 0-5 VDC output, 11-28 VDS input) provides pressure measurement capability by registering the axial force applied on the pushrod. During normal operation, the piston o-rings are lubricated so frictional forces are

only a small component of the measured force, and the push-rod transducer provides a reasonably accurate determination of pressure in the reservoir. For safety, the total force applied by the pushrod is limited by a shear membrane on the follower block as shown in Figure 2. The entire assembly of support frame, motor, drive train, and pressure tube is shown without the MRI magnet in Figure 3.

Non-metallic components in the central region of the magnet include the piston (Delrin), pressure tube (epoxy-glass fiber wrapped Plexiglass), contraction insert (Plexiglass) and plastic support column (Delrin). These parts, when assembled, sit atop an aluminum support tube that transfers the piston force to a bottom plate attached to frame crossmembers that run underneath the magnet.

Figure 4 depicts the piston design. A central bleed hole allows air to be expelled while loading the piston into the fluid-filled pressure tube. The bleed hole is plugged with a screw prior to application of the push rod. Multiple o-rings and wipers are designed to effectively seal the piston against internal pressures. The piston is shown in Figure 5 along with various o-ringed contraction inserts and the Delrin support tube.

The pressure tube has an internal diameter of 2 inches. The maximum height available for fluid in the reservoir section of the tube depends on the contraction and support tube inserts used. It is typically about 5.5 inches. In addition to the requirement to be non-metallic, the tube had to present a smooth surface to the piston o-rings and sufficient strength and ductility for the anticipated internal pressures and pressurization rates. The overall clearance available for the tube limited its wall thickness to less than 0.34 inch. These requirements lead us to choose a fiber-epoxy reinforced Plexiglass tube with the fiber reinforcement bonded to the outside of the tube. Glass fibers wetted with a room-temperature cure epoxy resin were wound in a circumferential manner around a Plexiglass tube of appropriate diameter. The inside of the tube was machined to the final inner diameter.

A simple model based on analytical formulae was used to predict the stresses and radial displacements of the fiber-epoxy overwrapped Plexiglass tube under internal pressure loads. The model was used in the selection of appropriate fiber and epoxy type, fiber content, and reinforcement thickness and to ensure sufficient hoop strength to resist up the maximum internal pressure with an adequate safety margin (factor of 5). The model used boundary displacement matching to analyze the combination of the inner Plexiglass cylinder and the outer fiberglass overwrap.

For a cylinder of inner radius a and outer radius b under internal pressure P_{int} , the hoop stress S_2 equals:

$$s_2 = -p_{\text{int}} \frac{a^2(b^2 + r^2)}{r^2(b^2 - a^2)} \quad (1)$$

while the radial stress s_3 equals:

$$s_3 = p_{\text{int}} \frac{a^2(b^2 - r^2)}{r^2(b^2 - a^2)} \quad (2)$$

The radial displacement at the inner radius equals:

$$\Delta a = -p_{\text{int}} \frac{a}{E} \left(\frac{b^2 + a^2}{b^2 - a^2} + \nu \right) \quad (3)$$

where ν is Poisson's ration. The radial displacement at the outer radius equals:

$$\Delta b = -p_{\text{int}} \frac{b}{E} \left(\frac{2a^2}{b^2 - a^2} \right) \quad (4)$$

For a cylinder under external pressure p_{ext} , the corresponding equations are:

$$s_2 = p_{\text{ext}} \frac{b^2(a^2 + r^2)}{r^2(b^2 - a^2)} \quad (5)$$

$$s_3 = p_{\text{ext}} \frac{b^2(r^2 - a^2)}{r^2(b^2 - a^2)} \quad (6)$$

$$\Delta a = p_{\text{ext}} \frac{a}{E} \left(\frac{2b^2}{b^2 - a^2} \right) \quad (7)$$

$$\Delta b = p_{\text{ext}} \frac{b}{E} \left(\frac{a^2 + b^2}{b^2 - a^2} - \nu \right) \quad (8)$$

These equations were solved to minimize the difference in radial displacements at the inner interface between Plexiglass and fiberglass epoxy using a Microsoft Excel program running on a Power Macintosh. The program was used to estimate the thickness of fiberglass-epoxy overwrap required for our application. A wall thickness of 1/16 inch was used for the Plexiglass based on availability of stock materials. From the known moduli and tensile strengths for Plexiglass and fiberglass epoxy (with 46 volume percent fiber) and the wall thickness for Plexiglass, it was determined that an overwrap consisting of 1/16 inch of fiberglass/epoxy would hold the tensile stresses in all materials to their safe

working stresses (ultimate tensile strength / safety factor). At 1000 psi. internal pressure, the working stress in the Plexiglass is 1261 psi. against a strength of 7500 psi.

Hoop strains predicted by this procedure were compared to actual hoop strains measured during hydraulic pressurization of the tube by microstrain gauges bonded to the outer epoxy surface. The agreement was reasonably good, and the measured strains varied linearly and reproducibly up to the maximum working pressure.

PROCESS STUDY

Process studies were performed to determine the conditions that lead to undesirable behavior (unstable or uncontrollably rising pressure). These studies involved variations in the following variables: base fluid viscosity, particle volume fraction, flow rate, and contraction ratio. The push rod load was monitored as material was forced through the contraction. This load data is easily converted to give the reservoir pressure versus piston position. Samples of material were collected from various regions (e.g. conical portion of contraction) and analyzed for particle content. The conical region of the contraction was imaged by proton MRI to examine the state of suspension for conditions that indicated possible particle jamming.

In all studies the base suspension fluid consisted of a mixture of UCON polyether oil, ammonium nitrate, water, and ethylene glycol in appropriate ratios to match the density of the suspended particles. Each base fluid was Newtonian, i.e. constant viscosity versus shear rate. The suspensions are shear thinning. The particles were polymethyl methacrylate (PMMA) and had an average diameter of 600 micrometers.

Pressure Trace Data

Figure 6 shows pressure versus piston position traces for suspensions with a relatively high base fluid viscosity (27 poise) and an 8:1 contraction ratio. Three types of curves are seen, and this behavior is typical of all the traces observed with this base fluid viscosity. At the lowest particle concentration (61.0 vol %) the pressure remains low and fairly constant throughout the run. At 62.6% particles the pressure is somewhat higher and approximately constant initially but suddenly increases dramatically near the end of the run. At the highest concentration (63.3%) the pressure rises throughout the run and reaches very high levels. Thus, small changes in the starting particle concentration lead to large differences in processing behavior. The traces at 62.6% and 63.3% are representative of undesirable situations for injection loading processes. Generally, we found that whenever the initial particle concentration was above 62%, peaks or rising curves were observed in the pressure-position traces and the behavior indicated a very critical sensitivity to particle concentration. This statement is true for all the different base fluid viscosities studied.

With a 4:1 contraction ratio we did not observe rising or peaked pressure traces, indicating that reducing the contraction ratio reduces the tendency for particle jamming.

Table 1 lists observations for the runs with the 27-poise base fluid. In this table, steady pressure refers to the average pressure in any relatively constant pressure portion of the trace. Peak pressure refers to the maximum pressure in the trace. Samples were taken from the suspension as loaded and from the conical portion of the contraction following each run. These sample were analyzed for particle concentration, and the results are reported in Table 1.

Table 1. Pressure Trace Observations and Suspension Concentrations for 27-Poise Base Fluid Runs.

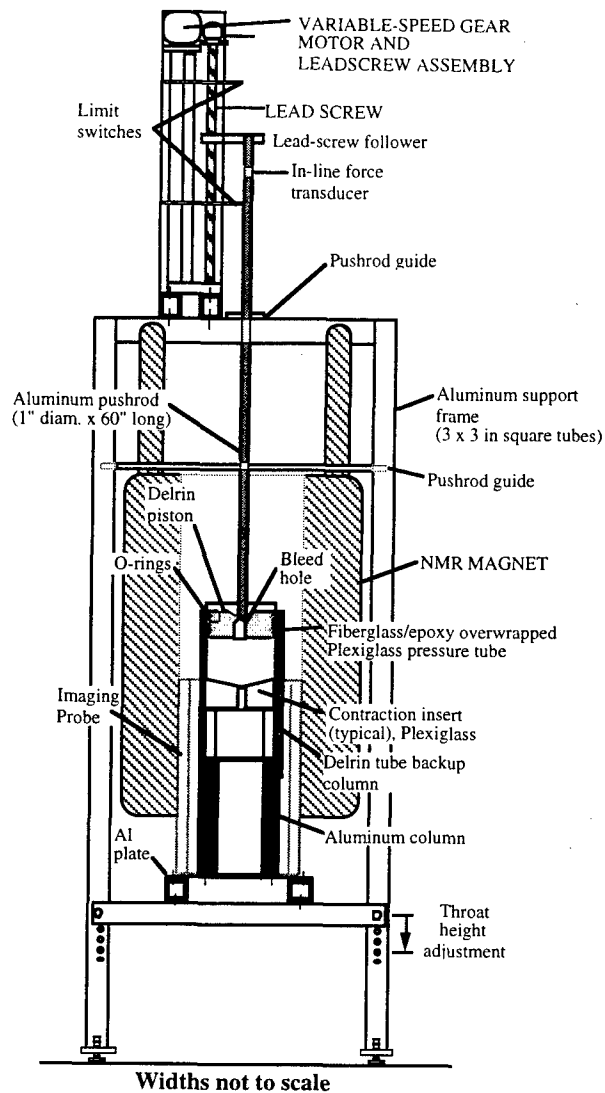
PISTON VELOCITY (in/s X 10²)	START CONC (%)	CONE CONC (%)	STEADY PRESS (psi)	PEAK PRESS (psi)	P vs Position Shape
1.93	61.0	54.8	7	9	Flat
0.69	61.1	55.0	5	7	Flat
3.33	61.2	55.9	13	14	Flat
0.69	61.5	60.0	9	11	Flat
3.25	63.1	59.7	20	23	Flat
0.66	63.2	63.5	10	12	Flat
1.91	61.9	68.4	16	76	Peaked
3.25	62.1	68.9	30	255	Peaked
1.87	62.6	66.2	16	70	Peaked
0.67	63.3	67.8	10	25	Peaked
1.79	63.3	69.6	----	365	Rising
3.26	63.4	70.9	----	420	Rising

Table 1 indicates that whenever peaked or rising pressure traces are observed, the particle concentration in the cone at the end of the run is higher than the starting concentration. Apparently, for these cases the process has caused a relative increase in particle concentration in the cone. These end concentrations are approaching maximum packing, so this observation is consistent with formation of a particle mat in the contraction region as argued from the NSW and SIT process studies. This phenomenon seems to be driven by the initial particle concentration, contraction ratio, and flow rate. Generally, it is observed when initial particle concentration is above 62% and at the higher flow rates.

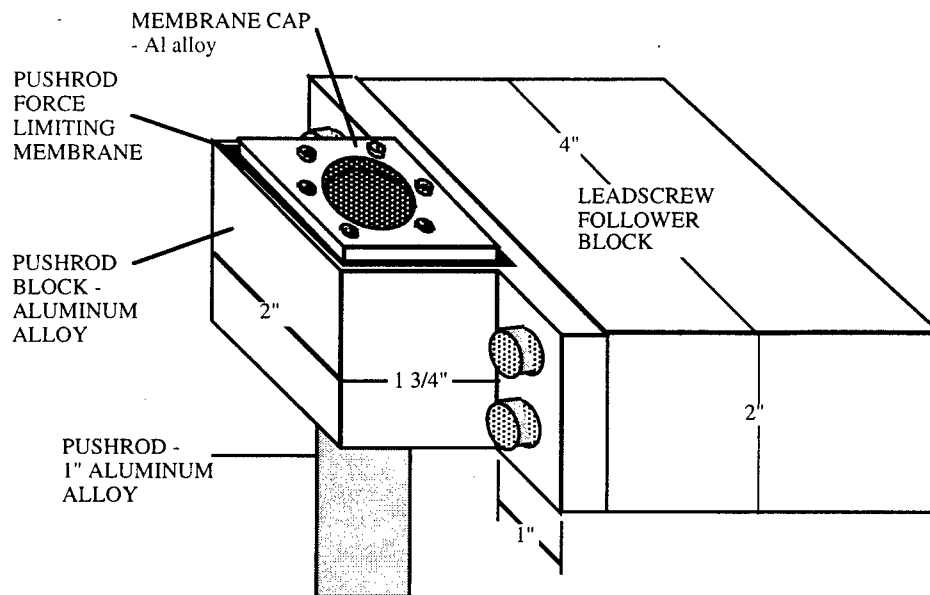
MRI Data

Proton MR Images of the contraction region of the 8:1 insert for a run in which the pressure rose to a peak are shown in Figure 7. The left image was taken with the piston near top of reservoir, and in the right image after the piston moved to the bottom of reservoir. These fluid-fraction images show how particles are distributed within the contraction. (Darker pixels correspond to volume excluded by the particles, hence pixel intensity gives a measure of local particle concentration.) The overall average pixel intensity is slightly higher in the right hand image of Figure 7, but the standard deviation of pixel intensity on the right is 50% greater. Differences are more easily discernible in the close up views and pixel intensity histograms shown in Figure 8. In this view, the histogram peak is at a slightly lower intensity for the post-process image (right). The broader distribution of pixel intensities is clearly evident in the right histogram. These statistical results indicate that the distribution of particles and suspending fluid is less uniform after the run than in the initial mix, consistent with clumping or agglomeration of particles in the contraction. With MRI, we have obtained a direct view into the state of the suspension during undesirable processing behavior.

The model injection loader can be used in future studies to understand these phenomena in more depth. Its modular design will allow exploration of the many possible options for process geometries. As a tool for the study of flows in contractions and tubes under high pressure it may be useful even outside the realm of propellant or explosives processing.

**FIGURE 1**

Schematic of model injection loader system.

**FIGURE 2**

Detailed schematic of follower block arrangement showing shear membrane employed for safety purposes.

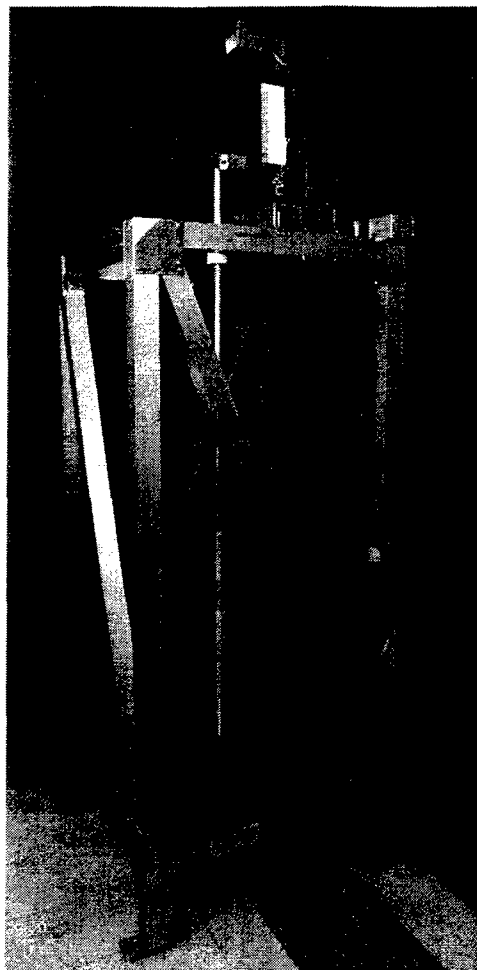


FIGURE 3

Photo of support scaffold with motor drive and pressure tube.

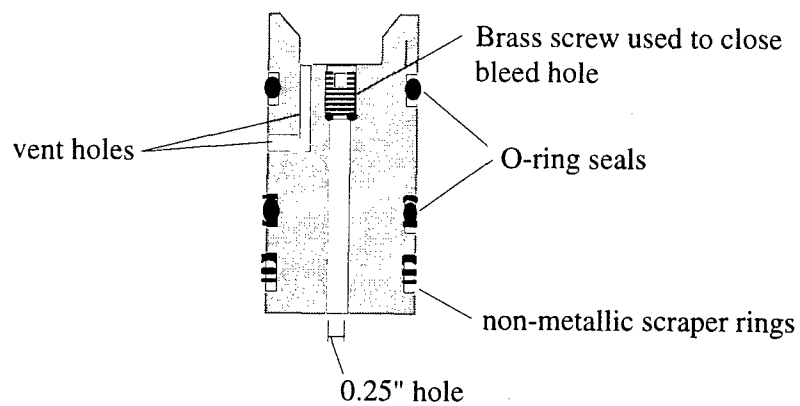


FIGURE 4

Schematic of piston.

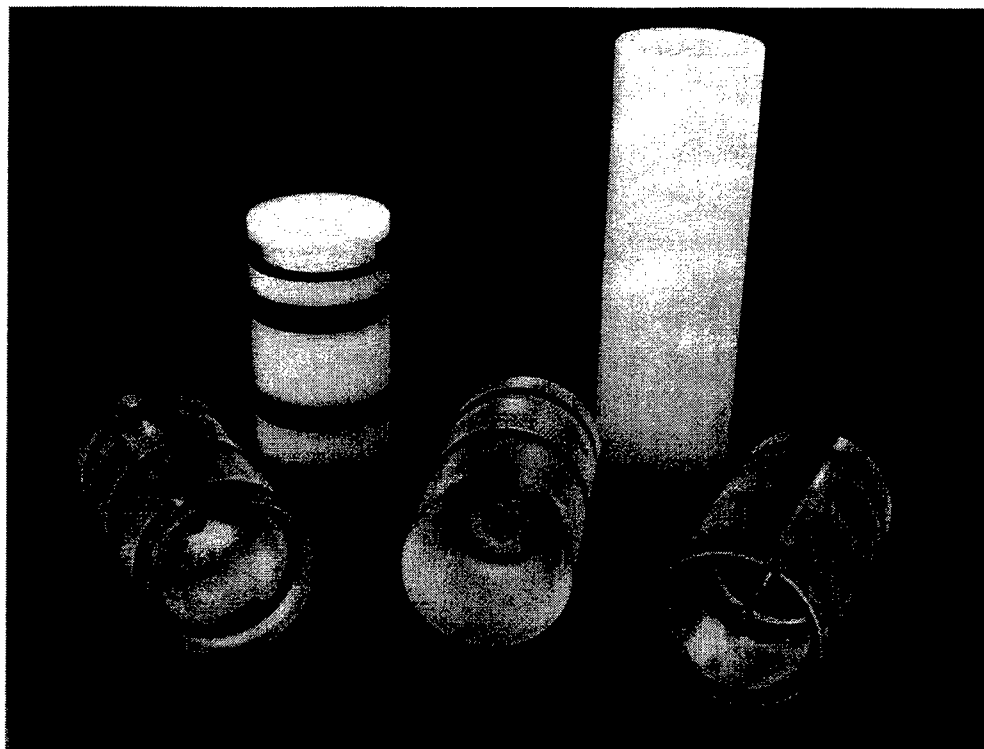
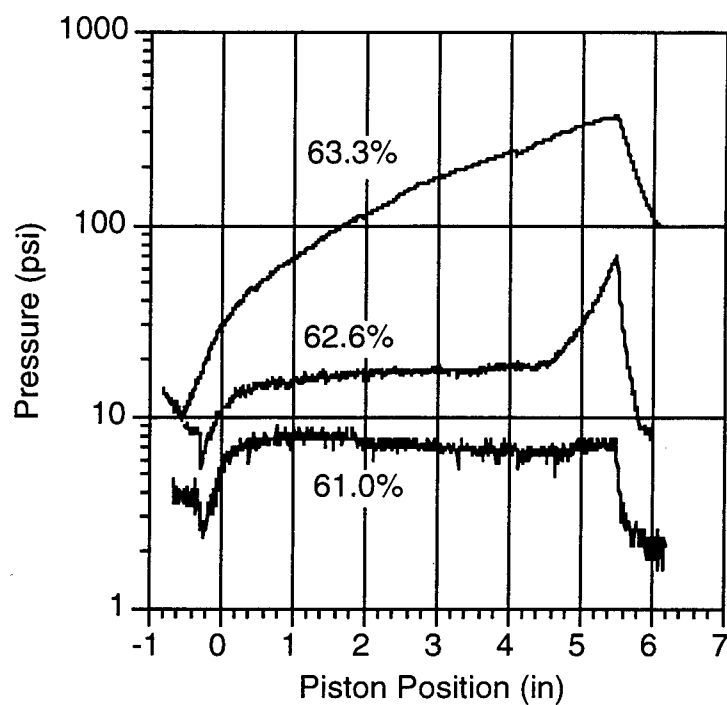


FIGURE 5

Photo of contraction inserts (foreground) and the Delrin support tube piston (background).

**FIGURE 6**

Plot of pressure versus piston position for three runs of the suspension made with a 27-poise base fluid through an 8:1 contraction. Piston velocity = 1.93, 1.87, and 1.79 inch/s, for the runs at 61.0%, 62.6%, and 63.3% starting particle concentrations, respectively.

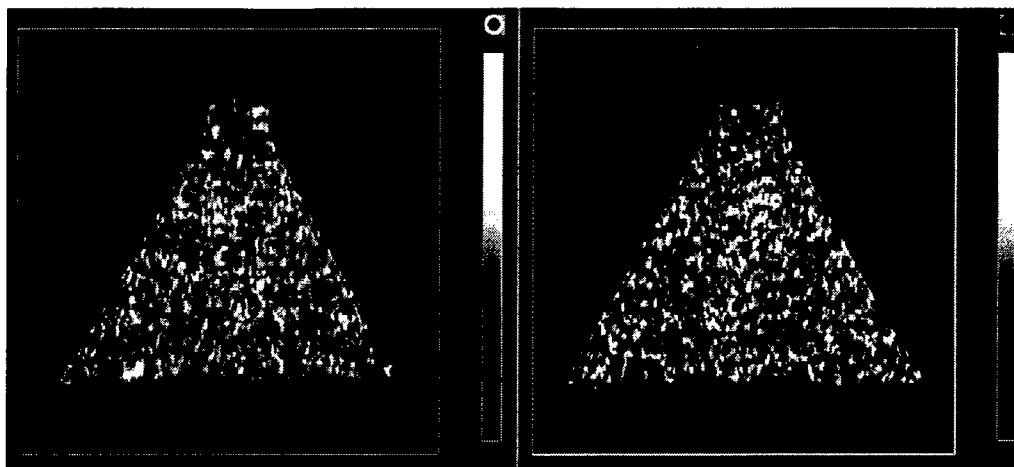


FIGURE 7

Proton magnetic resonance images of the fluid fraction in the conical section of the flow for the 8:1 contraction insert. Left image: Piston near top of reservoir. Right image: after piston displaced to bottom of reservoir. Data processing causes these images to be oriented with the flow direction upwards.

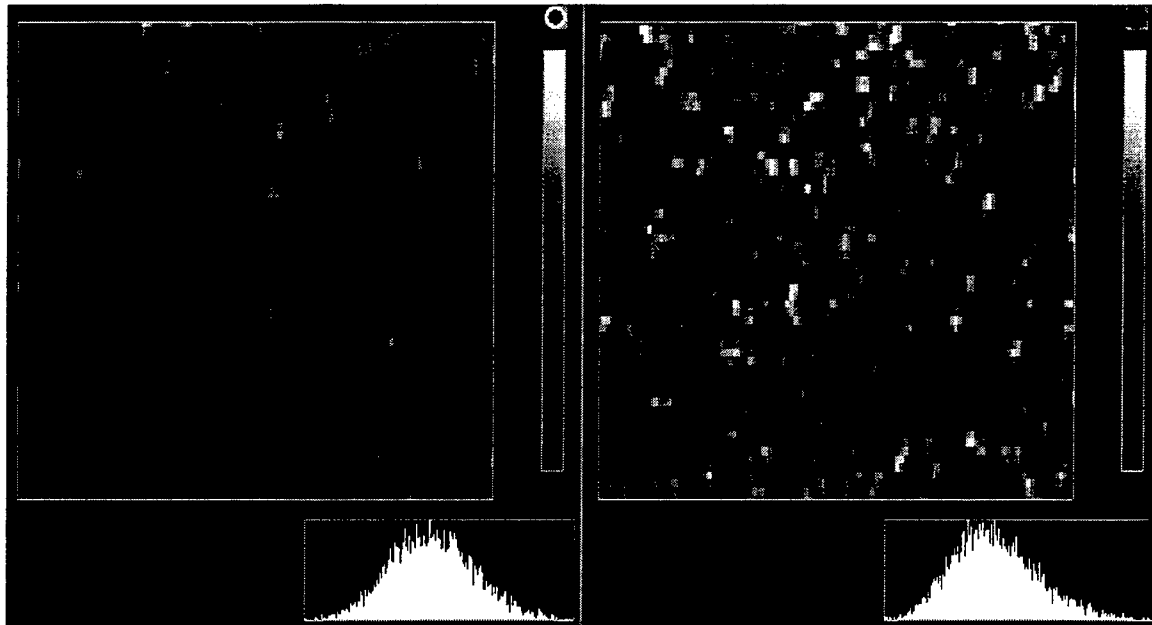


FIGURE 8.

Expansions of the images shown in Figure 7. The histograms at the bottom depict the distribution of pixel intensities in the regions viewed in the images.



DEPARTMENT OF THE NAVY

OFFICE OF NAVAL RESEARCH
800 NORTH QUINCY STREET
ARLINGTON, VA 22217-5660

IN REPLY REFER TO
5500/1
Ser 93/573
10 Jun 98

From: Chief of Naval Research
To: Director, Defense Technical Information Center,
ATTN: DTIC-FDRB

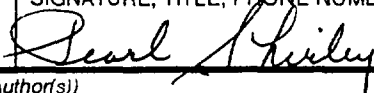

Subj: CHANGE OF ASSIGNED DISTRIBUTION STATEMENT ON TECHNICAL
REPORT AD B232385, Clean, Agile Processing Technology,
Final Report, December 1997, Lockheed Martin Missiles and
Space Company, Sunnyvale, CA

1. It is requested that Distribution Statement F on subject report be changed to Distribution Statement A.
2. Questions may be referred to the undersigned on 703/696-4620.

A handwritten signature in cursive script, reading "Ruth F. Kent", is positioned above the typed name.

RUTH F. KENT
By direction

EMBASSY REQUEST

DEFENSE TECHNICAL INFORMATION CENTER REQUEST FOR RELEASE OF LIMITED DOCUMENT NOTE: This form may be classified if necessary. See Instructions on reverse.		DTIC CONTROL NO. F8138002		USER ROUTING 507889	
SECTION I	REQUESTING ORGANIZATION AND ADDRESS The Canadian Embassy Canadian Defence Research and Development (CDRD)/CDLS(W) 501 Pennsylvania Avenue NW Washington DC 20001-2114		DTIC USER CODE NO. 20003		DATE OF REQUEST 11 May 98
			TYPE COPY AND QUANTITY <input checked="" type="checkbox"/> Paper Copy <u>1</u> Copy(s) <input type="checkbox"/> Microform _____ Copy(s)		
SECTION II			METHOD OF PAYMENT (X ONE) <input type="checkbox"/> Charge to NTIS Deposit Account No. <u>97222</u> <input type="checkbox"/> Bill My Organization to the Attention of: _____		
			SIGNATURE, TITLE, PHONE NUMBER OF REQUESTING OFFICIAL  (202) 682-7657		
SECTION III	AD NUMBER	BIBLIOGRAPHY (Title, Report Number, Author(s))			
	'ADB232385' UNCLAS	Clean, Agile Processing Technology. Sinton, S. W.			
SECTION IV	REQUIRED FOR (Explain need in detail) This document is requested by the Canadian Department of National Defence on behalf of the Directorate of Ammunition Program Management Engineering Services - DAPM(ES). The requester is the Ammunition Engineer at DAPM(ES) and is responsible for environmental aspects of ammunition and explosives operations in the Canadian Forces. As such, review of other countries' efforts and standards in the area of reduction and control of manufacturing effluent will contribute to building a knowledge base and improve the Canadian Forces international contributions. This information is of the type usually exchanged through channels such as TTCP.				
SECTION V	RELEASING AGENCY (Use Post Office Address Format!) Office of Naval Research, 800 N. Quincy St., Arlington, VA 22217-5660		RELEASING AGENCY DECISION <input checked="" type="checkbox"/> APPROVED FOR RELEASE TO THE ABOVE REQUESTER. DOCUMENT TO BE PROVIDED BY RELEASING AUTHORITY. <input type="checkbox"/> SANITIZED - PART OF TEXT REMOVED. DOCUMENT TO BE PROVIDED BY RELEASING AUTHORITY. <input type="checkbox"/> SANITIZED - DISTRIBUTION LIST AND BIBLIOGRAPHY REMOVED. DOCUMENT TO BE PROVIDED BY RELEASING AUTHORITY. <input type="checkbox"/> DISAPPROVED. REASON FOR DISAPPROVAL. <input type="checkbox"/> _____ RELEASED UNDER EXCHANGE AGREEMENT.		
	TYPED NAME AND TITLE OF RELEASING OFFICIAL PEGGY LAMBERT SECURITY MANAGER		TELEPHONE NO. 703/696-4620		SIGNATURE  RUTH F. KENT, SECURITY SPECIALIST FOR PEGGY LAMBERT
				DATE 980610	